3
HfO_2/TiO_2 Spherical Nanoparticles for Visible Photocatalytic Water Remediation of Industrial Dyes

The work described in this chapter has been published in *Materials Letters, 2018, 231, 225–228* and *RSC Advances, 2016, 6 (82), 78768-78773*

Hydrogenated HfO_2 doped TiO_2 (H-HfO_2/TiO_2), HfO_2 doped TiO_2 (HfO_2/TiO_2) and TiO_2 (pristine) were synthesized by a sol-gel and hydrothermal approach to demonstrate dye degradation of five different dyes – methylene blue (MB), methyl orange (MO), cresol red (CR), thymol blue (TB) and Solochrome black (SB). In this work, we have proposed a mechanism of assembling a core-shell structured TiO_2, initially doped with HfO_2 and then introducing hydrogen to engineer the bandgap and maximize the absorption for photocatalytic degradation of the aforementioned dyes. It was found that the MB degradation attained the best degradation efficiency of 90%, 10 min after the start of the reaction which can be attributed to good photocatalytic adsorption and degradation on the TiO_2 surface. Moreover, hydrogenation lead to the creation of mid-bandgap states increasing the adsorption ability of the catalysts used. The synthesized materials have been characterized using XRD and XRF to confirm the incorporation of HfO_2 on the TiO_2 lattice. Transmission Electron Microscope (TEM) was used for analysing the morphology and shape of the nanomaterials formed. Effect of photodegradation was studied using five different common dyes namely – methyl orange (MO), methyl blue (MB), cresol red (CR), thymol blue (TB) and solochrome black (SB).

3.1 Experimental section

3.1.1 Synthesis of HfO_2/TiO_2 spherical nanoparticles

Hydrogenated HfO_2 doped TiO_2 nano-spherical structures were synthesized following a two-step, sol-gel and solvothermal process.(Laishram, Shejale et al. 2016, Laishram, Shejale et al. 2018) Briefly, precursors of Ti and Hf, titanium tetra isopropoxide and hafnium isopropoxide (1% doping) were added dropwise to a solution containing a structure directing, hexadecyl amine, and ethanol. This milky white suspension is aged for a period of 18 hours to obtain a smooth-surfaced precursor bead. The precursor beads are further utilized in a solvothermal process to form nano-spherical structures of HfO_2 doped TiO_2 with a rougher and granular surface. The obtained nano-spheroids were lastly annealed under reducing atmosphere of hydrogen to obtain H-HfO_2/TiO_2. For comparison, undoped TiO_2 and HfO_2 doped TiO_2 annealed under the air atmosphere, HfO_2/TiO_2 were also synthesized.

3.1.2 Photocatalytic degradation using HfO_2/TiO_2 spherical nanoparticles

The dyes - methyl orange, methylene blue, cresol red, solochrome black and thymol blue were purchased from Acros, SRL, Sigma, and Qualigens. The dye solutions in water (20 μM) were prepared and 400 mg/L of each of the catalysts were dispersed in 15 mL of each of the dye solutions. All the photocatalysts were stirred for 30 minutes under dark conditions to establish an adsorption-desorption equilibrium of the dyes on the catalyst. The photocatalytic behaviour was observed by exposing the solutions with photocatalysts under 1 Sun simulated light (SS50AAA Solar Simulator, PET Photo Emission Tech., Inc.) for 50 min under mild stirring. For each sample monitoring, the residual concentration of the dye was estimated using a colorimeter (Fisher Scientific, Model No. 45). The amount of degradation was calculated from the initial dye concentration C_o and the final concentration C by using the Beer Lambert's equation,

$$\% \text{ Degradation} = (C_o\text{-}C)/C_o \times 100$$

3.2 Results and discussion

3.2.1 Structural and Morphological characterization

The material showed lattice planes distinct to anatase phase of TiO_2 which is identified with JCPDS 021-1272 (Figure 3.1a). No extra peaks were observed in the diffraction pattern of TiO_2 SNP and thus it can be concluded that the material synthesized is highly pure (Su, Yang et al. 2015). HfO_2/TiO_2 and H-HfO_2/TiO_2 showed broad hump at 28.3° and 31.62° ascertained to monoclinic HfO_2 (Wan and Zhou 2017). The effect on strain and crystallite size upon doping HfO_2 and eventual hydrogenation are observed and tabulated in Figure 3.1b and Table 3.1. The magnified (101) highest intense peak (Figure 3.1b) showed 2θ shift in the lower angle corresponding to ~0.04° and ~0.128° after doping HfO_2 and hydrogenation correspondingly. XRF plot in Figure 3.1c indicates presence of Hf ($L_{\alpha1}$ and $L_{\beta1}$) and Ti ($K_{\alpha1}$ and $K_{\beta1}$) in the synthesized of nanospheroids (SNP).

Lattice expansion of 0.0738% was observed for H-HfO_2/TiO_2 due to incorporation of bigger size HfO_2 on the TiO_2 lattice (Wang, Tan et al. 2016). Moreover, annealing under reducing hydrogen atmosphere creates defects in lattice contributing substantially to lattice expansion (Chen, Liu et al. 2011). The XRF spectroscopy is a non-destructive analysis technique that gives quantitative and qualitative assessment of elements. The intense peak showed the presence of larger amount of Ti in the sample and Hf as smaller humps due to 1% doping in the prepared SNP.

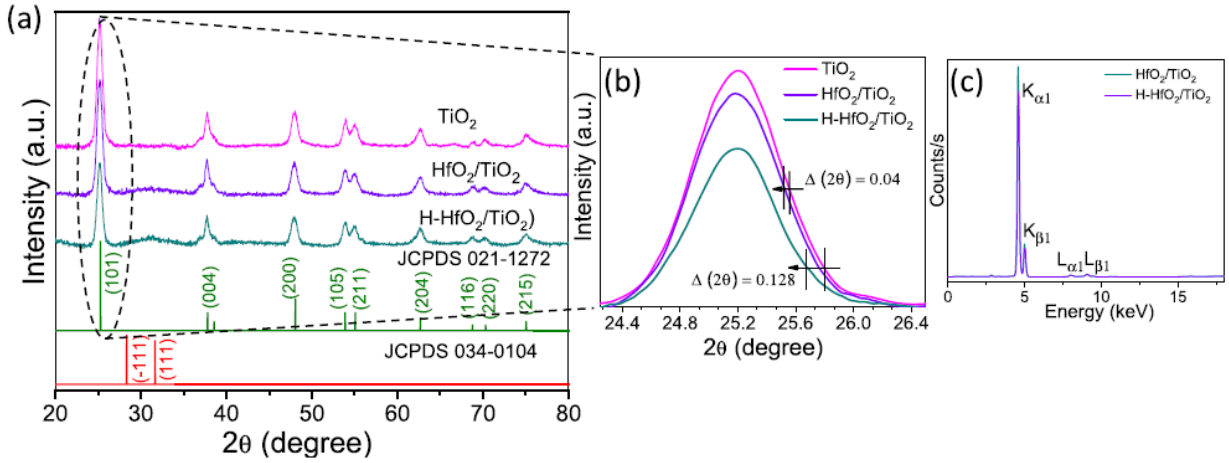

Figure 3.1: (a) XRD of the material with JCPDS data (b) XRD of highest intense peak (101) denoting shift and intensity change. (c) XRF spectra of doped TiO_2.

Table 3.1: Cell parameters of the synthesized SNP.

Sl. No.	*Synthesized SNP*	*Crystallite Size (in nm)*	*Strain*	*Unit cell parameter calculated*	
				a (nm)	*c (nm)*
1.	TiO_2	3.2018	0.5259 ± 0.2351	0.37889	0.88146
2.	HfO_2/TiO_2	3.0188	0.4137 ± 0.25294	0.37904	0.97097
3.	H- HfO_2/TiO_2	3.4863	0.5272 ± 0.2144	0.37917	0.97153

The uniformly formed spherical morphology of the synthesized materials was confirmed using TEM (Transmission Electron Microscope) as shown in Figure 3.2a-c. The TEM image clearly shows that TiO_2 spheroid is composed of grain-like particles of TiO_2 and HfO_2. The inset of Figure 3.2a-c revealed the gradual increase in the size of the spheroids upon doping with H-HfO_2/TiO_2 being the largest among all. The average diameter follows the order - TiO_2 (~305 nm) < HfO_2/TiO_2 (~326 nm) < H-HfO_2/TiO_2 (~400 nm). Also, the even distribution of pores can be observed by the light and dark contrast of TEM images. The HR-TEM images in Figure 3.2d-f indicate lattice spacing corresponding to that of the anatase phase of TiO_2 with an average d-spacing value of 0.35 nm consistent to the (101) plane as observed in the XRD pattern

(Figure 3.1a). But due to the doping, there is a small decrease in the lattice spacing as indicated in Figure 3.1b. The bright spots in the SAED (Selected Area Electron Diffraction) pattern in Figure 3.2g-h are fainted upon hydrogen treatment due to a slight decrease in polycrystalline nature which is understandable.

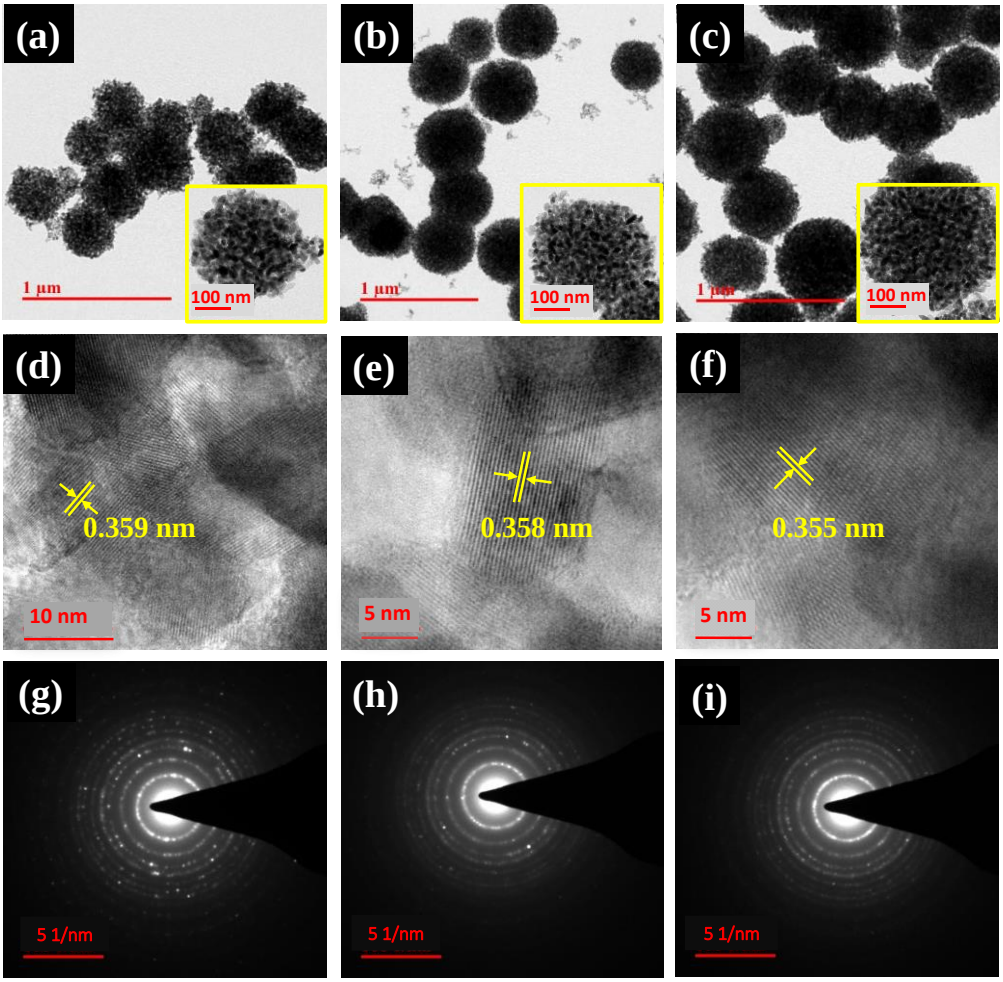

Figure. 3.2: TEM images, HR-TEM images and the SAED images of pristine TiO_2 (a, d, g) HfO_2/TiO_2 (b, e, h) and (c, f, i) H-HfO_2/TiO_2. The inset of a, b and c show the respective spherical structure.

3.2.2 Photocatalytic activity

The aqueous solution of various dyes namely, MB, CR, MO, TB and SB were degraded under 1 sun solar simulation using 400 mg/L of the catalyst. The photocatalytic degradation activity was carried out for all the synthesized materials as given in Figure 3.3a-c for TiO_2, HfO_2/TiO_2 and H-HfO_2/TiO_2 respectively. It can be observed that amongst all the dyes, methylene blue is best degraded by all the three catalyst whereby the degradation time was shortest for the hydrogenated HfO_2/TiO_2 by degrading 90% of the dye effectively within the first 10 min. MB shows strong absorbance at 664 nm and 292 nm with a shoulder peak at 614 nm and 245 nm (Figure 3.3d–f). The adsorption of dye upon the catalyst surface depends on the electrostatic interaction between the dye and surface of the catalyst (Wang, Tan et al. 2016). TiO_2 is amphoteric and reacts differently with pH, e.g. MB is cationic and adsorption is stronger with TiO_2 surface leading to higher degradation efficiency under basic conditions (Figure 3.3d–f). The catalyst containing dye gets degraded when electron-hole pair generated by the light reacts with water molecules to yield active radicals. The oxidation of dyes leads to cleavage of bonds and breaking of aromatic rings with formation of smaller inorganic molecules in three steps– decolourization, degradation and mineralization.

Each of the photocatalytic degradation studies using the respective catalysts was performed for 50 min. It was observed that for the case using the undoped TiO_2, degradation of methylene blue was found to be the best with 90% of the dye degrading after 40 min of starting

the reaction. While methyl orange was degraded least by degrading 60% at the end of the reaction at 50 min. Gradual degradation was observed for cresol red, degrading 90% at the end of the reaction at 50 min by TiO_2. The effective degradation for all the dyes using undoped TiO_2 as photocatalyst is as follows MB > CR > TB > SB > MO. Doping of HfO_2 over TiO_2 showed similar photocatalytic degradation to that of TiO_2 with the catalyst showing superior activity for MB degradation advancing the reaction time by 20 min for 90% degradation efficiency. Interestingly, when the HfO_2 doped TiO_2 is hydrogenated it was observed that the degradation was achieved much faster with higher degree of activity. For example, MB was degraded by 90% 10 min after the start of the reaction while for SB, 70% degradation was achieved after 25 min. Moreover, the extent of degradation for all the other dyes – TB, CR and MO were boosted and achieved almost 80-90% degradation by the end of the reaction at 50 min as otherwise observed in the previous two cases.

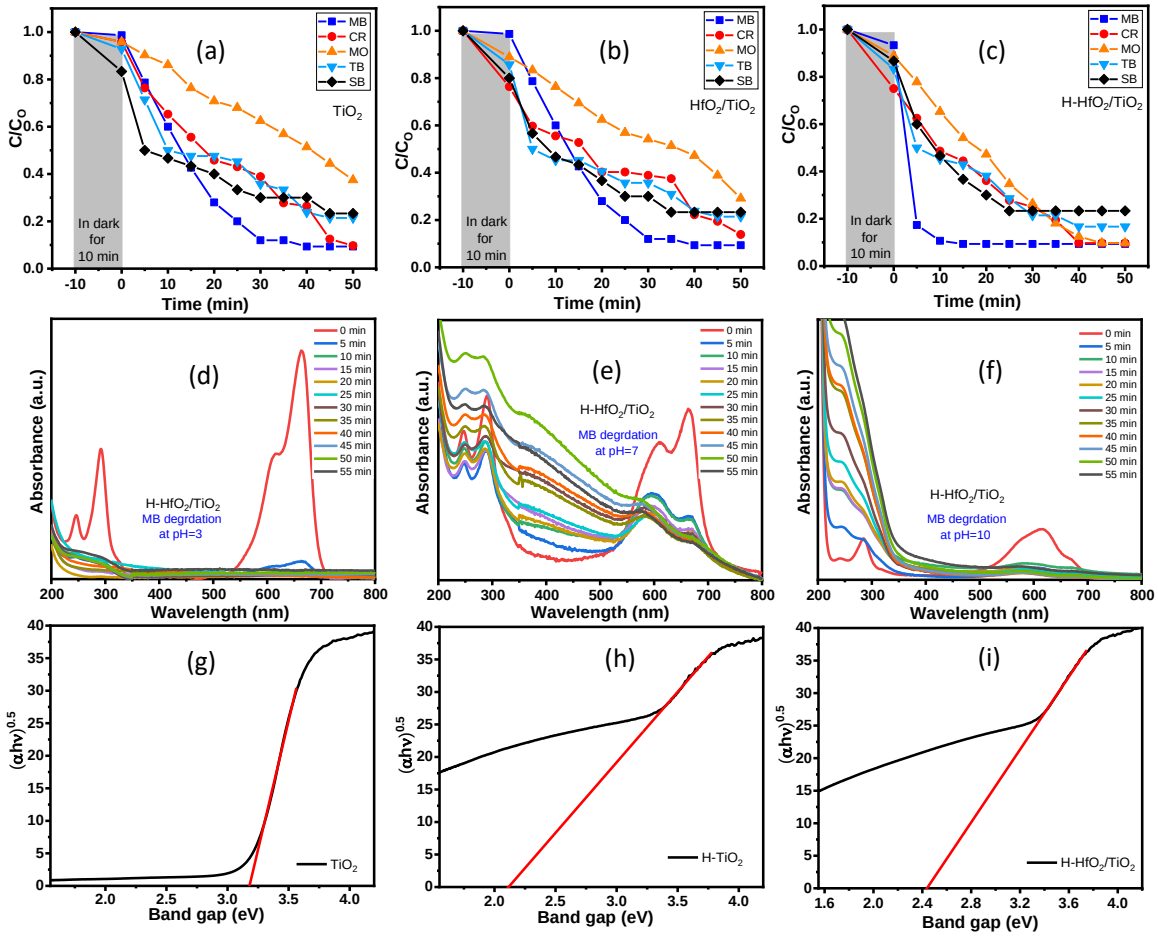

Figure. 3.3: (a–c) Degradation of five different dyes using TiO_2, HfO_2/TiO_2 and $H\text{-}HfO_2/TiO_2$ at pH 7. (d-f) show the degradation of MB dye at different pH using $H\text{-}HfO_2/TiO_2$. Tauc plot of TiO_2 (g), $H\text{-}TiO_2$ (h) and $H\text{-}HfO_2/TiO_2$ (i) respectively for bandgap estimation.

The enhanced degradation activity is due to the increase in absorption ability of the nanomaterial after hydrogenation beyond the UV region in the solar spectrum. It can be noted that TiO_2 with a bandgap of 3.18 eV, when annealed under hydrogen, decreases to 2.1 eV (1.8 eV reported in literature). When doped with 1% HfO_2, the bandgap changes minimally to 3.14 eV. Interestingly, when 1% HfO_2 is doped with TiO_2 and annealed under reducing atmosphere, the bandgap is tuned to 2.47 eV (Figure 3.3g–i). Tuning of bandgap is an important consideration to maintain a balanced trade-off between increasing absorption in solar spectrum and reducing the recombination of exciton pairs.

Moreover, these results showed successful incorporation of hydrogen into the lattice of TiO_2 which help in creating mid gap states between the bands of TiO_2 thereby decreasing the overall bandgap of TiO_2 (Chen, Liu et al. 2011, Zhang and Park 2017). The bandgap and the

optical property of the materials are given elsewhere (Laishram, Shejale et al. 2016). These processes all amount up to better utilization of the solar spectrum absorbing a greater number of photons. The % degradation activity of each dye using all the prepared photocatalyst was calculated and plotted in Figure 3.4a-e. The reaction rates for the best degraded MB for all the three catalyst were calculated (Table 3.2).

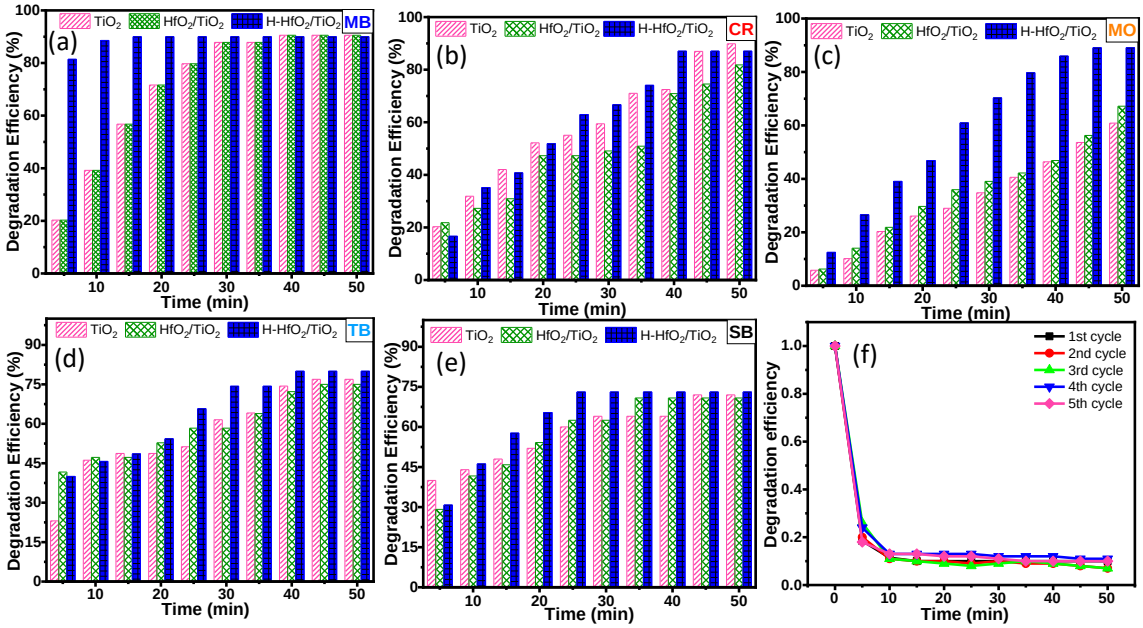

Figure. 3.4: Histogram plot of TiO_2, HfO_2/TiO_2 and $H\text{-}HfO_2/TiO_2$ showing different degradation efficiency of respective five dyes as indicated in the inset. (f) Plot of recyclability test for MB dye using $H\text{-}HfO_2/TiO_2$ as photocatalyst.

Table 3.2. Degradation activity of MB dye with different catalyst.

Sl. No.	Catalyst	Pollutant	R^2	K min^{-1}
1.	TiO_2	MB	0.94	0.053
2.	HfO_2/TiO_2		0.94	0.053
3.	$H\text{-}HfO_2/TiO_2$		0.90	0.216

The improved degradation efficiency using $H\text{-}HfO_2/TiO_2$ can be attributed to different factors. Firstly, the increased surface area provided by doping of both HfO_2 and hydrogenation leading to a highly mesoporous structure with high surface area for exchange of mass between the dye and catalyst molecules as confirmed from the BET analysis (Figure 3.5a-d, Table 3.3) (Panomsuwan, Watthanaphanit et al. 2015, Sambandam, Surenjan et al. 2015). TiO_2 and $H\text{-}TiO_2$ (Figure 3.5a, b) showed Type II isotherm with H3 type hysteresis while after doping with HfO_2, HfO_2/TiO_2 and $H\text{-}HfO_2/TiO_2$ (Figure 3.5c, d) showed Type V and H1 hysteresis isotherm according to the IUPAC classification. Thus, pristine and hydrogenated TiO_2 can be identified with non-porous or macroporous adsorbent along with slit-like pore structures. Whereas, doping with HfO_2 gave rise to H1 type hysteresis associated mostly with porous structures with well-defined cylindrical pores. Thus, hydrogen annealed HfO_2 doped, $H\text{-}HfO_2/TiO_2$ showed enhanced absorption in the solar spectrum due to the lowering of bandgap and its mesoporous nature of the pore structure leads to good dye-catalyst interaction giving high efficiency during photocatalytic dye degradation. Secondly, the reduction of bandgap due to hydrogenation promotes more exciton pair generation whereby the electrons helps the formation of superoxide radical and the holes oxidize the water molecules to form hydroxyl radicals. Thus, $H\text{-}HfO_2/TiO_2$ showed the highest degradation rate at 0.216 min^{-1} among the three catalysts tested with MB dye (Table 3.2). Also, the % degradation efficiency was calculated and plotted (Figure 3.4a-e) for each of the five dyes degraded using all catalysts. Recyclability test was performed for five cycles for MB with $H\text{-}HfO_2/TiO_2$, revealed high stability of catalyst (Figure 3.4f).

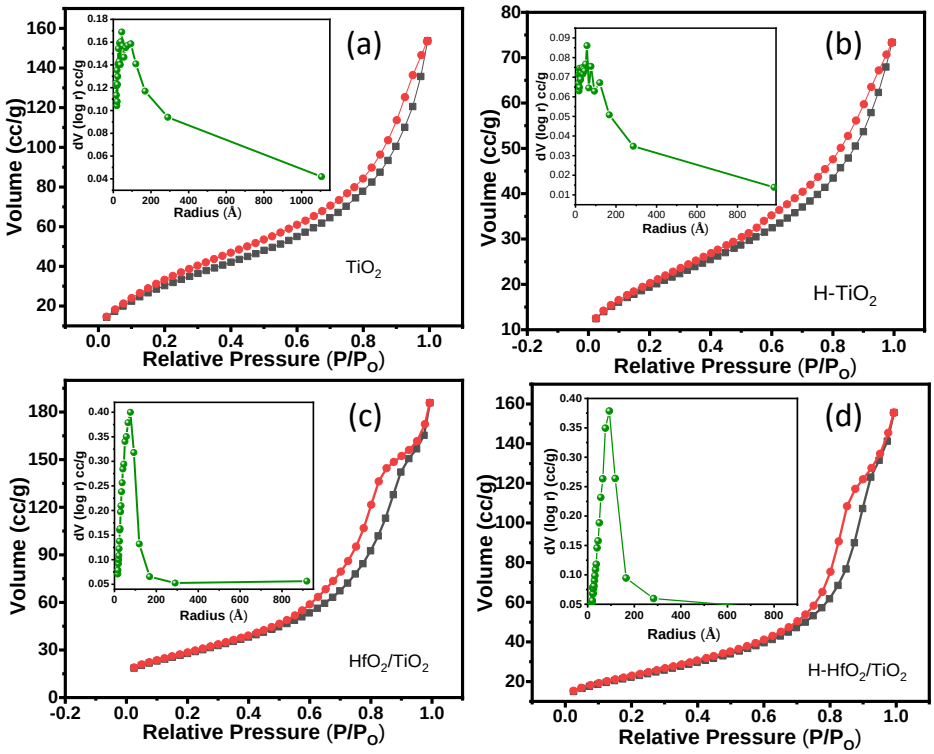

Figure. 3.5: Bet isotherm plots of pristine (a) TiO_2, (b) H-HfO_2/TiO_2, (c) H-HfO_2/TiO_2 and (d) H-HfO_2/TiO_2.

Table 3.3. Surface area analysis of all the samples.

Sl. No.	Sample Name	Surface area (m^2/g)	Pore Radius(Å)	Pore Volume (cc/g)	Types of Pore
1.	TiO_2	121.7	39.1	0.24	Macroporous and slit like pore
2.	H-TiO_2	70.59	32.1	0.11	Macroporous and slit like pore
3.	HfO_2/TiO_2	102.7	55.9	0.28	Mesoporous and cylindrical pore
4.	H-HfO_2/TiO_2	80.6	59.7	0.24	Mesoporous and cylindrical pore

Obliteration of dye to smaller molecules due to photocatalytic degradation can be realized by the appearance of new peaks at lower retention time in the HPLC chromatogram (Figure 3.6). HPLC 515 Pump equipped with Waters 2489 system was used for the analysis of the chromatographic separation of the MB dye solution. C18 was used for column separation with acetonitrile-water = 40:60 (v:v) as the mobile phase at 1 mL min^{-1} flow rate. The experimental data are for before and after degradation at 50 min. The degradation in the dye molecules can well be appreciated by the disappearance of MB peaks and the appearance of peaks at lower retention time. Finally, the doping induces defects and oxygen vacancies that acts as trapping sites decreasing the recombination rate(Panomsuwan, Watthanaphanit et al. 2015). Thus, the compound effect of doping HfO_2 over TiO_2 and subsequent annealing under H_2 atmosphere can be a suitable means to synthesize an advanced form of SNP for using in accelerated photocatalytic dye degradation applications.

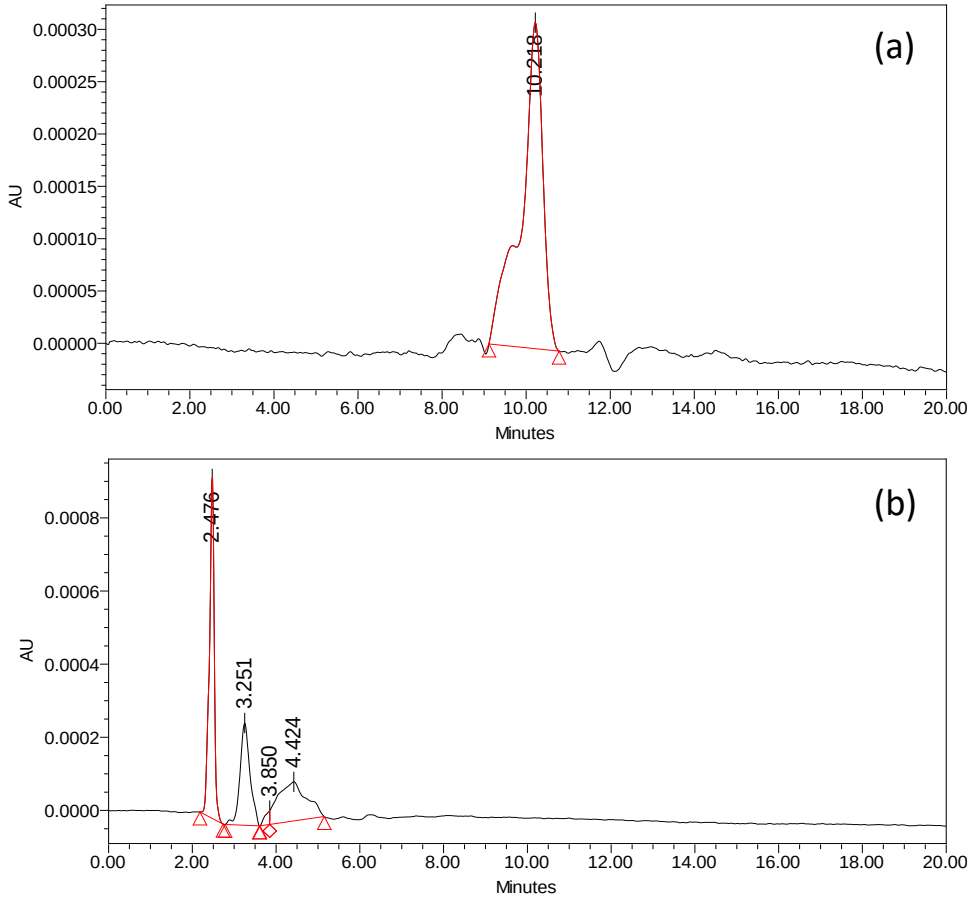

Figure. 3.6: HPLC chromatogram of MB dye before (a) and after (b) photocatalytic degradation using H-HfO_2/TiO_2 as photocatalyst.

3.3 Conclusion

Nano spherical composites of granular TiO_2 and HfO_2 are successfully synthesized in a sol-gel and hydrothermal process. Morphological study using TEM analysis revealed the granular composition of each nano-spherical to be a composition of grains of TiO_2 and HfO_2 which gives improved mesoporosity to the nanostructure. These nanospheroids provide good number of active surface sites and high surface area for dye attachment. Also, this nanostructure inherently due to its shape and composition help capture the incoming photons for an enhanced light scattering effect. Degradation activity of the five most commonly used dyes was compared and tested using the synthesized nanomaterial and found super-fast degradation for methylene blue and increased degradation activity for the remaining dyes.

...